THE JOURNAL OF BIOLOGICAL CHEMISTRY
Vol. 279, No. 30, Issue of July 23, pp. 31842–31853, 2004

Printed in U.S.A.

Molecular Dissection of Na^+ Binding to Thrombin*

Received for publication, February 17, 2004, and in revised form, April 14, 2004
Published, JBC Papers in Press, May 19, 2004, DOI 10.1074/jbc.M401756200

Agustin O. Pineda‡, Christopher J. Carrell, Leslie A. Bush, Swati Prasad, Sonia Caccia, Zhi-Wei Chen, F. Scott Mathews, and Enrico Di Cera§

From the Department of Biochemistry and Molecular Biophysics, Washington University School of Medicine, St. Louis, Missouri 63110

Na^+ binding near the primary specificity pocket of thrombin promotes the procoagulant, prothrombotic, and signaling functions of the enzyme. The effect is mediated allosterically by a communication between the Na^+ site and regions involved in substrate recognition. Using a panel of 78 Ala mutants of thrombin, we have mapped the allosteric core of residues that are energetically linked to Na^+ binding. These residues are Asp-189, Glu-217, Asp-222, and Tyr-225, all in close proximity to the bound Na^+. Among these residues, Asp-189 shares with Asp-221 the important function of transducing Na^+ binding into enhanced catalytic activity. None of the residues of exosite I, exosite II, or the 60-loop plays a significant role in Na^+ binding and allosteric transduction. X-ray crystal structures of the Na^+-free (slow) and Na^+-bound (fast) forms of thrombin, free or bound to the active site inhibitor H-D-Phe-Pro-Arg-chloromethylketone, document the conformational changes induced by Na^+ binding. The slow → fast transition results in formation of the Arg-187:Asp-222 ion pair, optimal orientation of Asp-189 and Ser-195 for substrate binding, and a significant shift of the side chain of Glu-192 linked to a rearrangement of the network of water molecules that connect the bound Na^+ to Ser-195 in the active site. The changes in the water network and the allosteric core explain the thermodynamic signatures linked to Na^+ binding and the mechanism of thrombin activation by Na^+. The role of the water network uncovered in this study establishes a new paradigm for the allosteric regulation of thrombin and other Na^+-activated enzymes involved in blood coagulation and the immune response.

Thrombin, the key serine protease responsible for blood coagulation (1, 2), vascular development, and signaling (3–5), is a Na^+-activated allosteric enzyme (6). This property is a variation on the common theme encountered within the large family of monovalent cation-activated enzymes that typically use K^+ as an activator (7, 8). Na^+ activation is also observed in other enzymes involved in blood coagulation and the immune response but not in digestive and degradative enzymes like trypsin and chymotrypsin (9). Notably, the emergence of this property during evolution played a significant role in the segregation of function in serine proteases (10, 11).

The Na^+ binding site of thrombin is strategically located in close proximity to the S1 pocket (12), nestled between the 220- and 186-loops that contribute to the primary specificity of serine proteases (13–15). The Na^+ binding sites of coagulation factor Xa (16) and activated protein C (17) are similarly located and arranged structurally. Binding of Na^+ to thrombin enhances the k_{cat}/K_m toward small chromogenic substrates by significantly increasing the rate of diffusion into the active site and the rate of acylation (6, 18). The effect is exquisitely allosteric because the Na^+ binding site is located away from residues of the catalytic triad or involved directly in substrate recognition. The binding of Na^+ also influences recognition of macromolecular substrates like fibrinogen and PAR1 and manifests itself physiologically as a significant procoagulant and prothrombotic effect (19, 20). Analogous procoagulant effects of Na^+ have been reported for factor Xa (21, 22). The synergism between thrombin and factor Xa in initiating and maintaining blood coagulation (1, 2) supports a key role for Na^+ in promoting blood clotting.

The physiologic importance of the Na^+ effect on thrombin is demonstrated by the bleeding phenotypes observed with prothrombins Frankfurt (23), Salakta (24), Greenville (25), and Scranton (26), where the mutations compromise Na^+ binding. Furthermore, changes in the Na^+ concentration of plasma resulting in hypernatremia ($[Na^+] > 145$ mM) or hyponatremia ($[Na^+] < 135$ mM) are among the most common electrolyte disorders encountered by primary care providers, nephrologists, and pediatricians (27, 28) and are often associated with thrombosis or bleeding, respectively (19). Even under physiologic conditions, the Na^+ concentration of plasma drops drastically around platelet thrombi *in vivo* (29), lending further support to the importance of Na^+ in controlling the roles of thrombin and other enzymes in blood coagulation and thrombosis.

Under physiologic conditions of $[Na^+]$ (140 mM), pH and temperature, the K_d for Na^+ binding to thrombin is 110 mM (6, 30, 31), which implies that nearly half of the thrombin molecules generated *in vivo* from prothrombin are in the Na^+-free slow form. This basic property of thrombin was discovered in 1992 (6), but since then the Protein Data Bank has accumulated >150 structures of the enzyme that, with only one exception, have been solved in the presence of Na^+ and portray thrombin in the fast form. The first and only structure of thrombin in the slow form was reported in 2002 (32). This is also the first structure of the enzyme solved in the absence of any active site or exosite ligands that bias the conformation in favor of the Na^+-bound fast form (33, 34). The structure of the free slow form, solved at 2.8-Å resolution, documents intriguing changes in the environment of Asp-189 and Ser-195, together with a paucity of water molecules in the vacant Na^+ site and

* This work was supported in part by National Institutes of Health Research Grants HL49413, HL58141, and HL73813. The costs of publication of this article were defrayed in part by the payment of page charges. This article must therefore be hereby marked "*advertisement*" in accordance with 18 U.S.C. Section 1734 solely to indicate this fact.

The atomic coordinates and structure factors (codes 1SGI, 1SG8, 1SHH, and 1SFQ) have been deposited in the Protein Data Bank, Research Collaboratory for Structural Bioinformatics, Rutgers University, New Brunswick, NJ (http://www.rcsb.org/).

‡ Recipient of a Fellowship from the American Heart Association.

§ To whom correspondence should be addressed. Tel.: 314-362-4185; Fax: 314-747-5354; E-mail: enrico@biochem.wustl.edu.

the neighbor primary specificity pocket (32). These changes are borne out by comparing the free slow form with the PPACK[1]-inhibited (35) or hirugen-inhibited (36) fast form of the enzyme. Important questions therefore remain as to whether the observed changes in the free slow form are due to the absence of Na^+ or PPACK and whether the lack of solvent in the water channel embedding the Na^+ site is an artifact due to the low resolution of the slow form structure. These questions are best addressed by solving the structures of thrombin in the four possible ligated intermediates with Na^+ and PPACK, which is a suicide inhibitor mimic of the specific chromogenic substrate of thrombin H-D-Phe-Pro-Arg-*p*-nitroanilide (FPR). A key reagent used for these studies is the thrombin mutant R77aA that abrogates the site of autoproteolytic cleavage in exosite I (37). That enables crystallization of the free form of the enzyme without introducing changes into active site residues, like Ser-195, that are now known to bear important signatures of the allosteric transition of the enzyme.

Here we present the high resolution structures of the four intermediates (free thrombin, thrombin bound to Na^+, thrombin bound to PPACK, thrombin bound to PPACK and Na^+) that define the detailed changes linked to Na^+ binding in the absence and presence of an active site ligand. In addition, we complement the structural investigation with an extensive Ala-scanning mutagenesis mapping of thrombin residues located in exosite I, exosite II, the 60-loop, the specificity sites S1–S4, and the Na^+ binding environment. The mapping identifies the allosteric core of residues energetically linked to Na^+ binding and the residues responsible for the Na^+-induced enhancement of catalytic activity toward the chromogenic substrate FPR, which is a relevant reporter of the interaction of the active site of thrombin with fibrinogen and PAR1 (38). The resulting functional and structural information offers unprecedented details on the molecular origin of thrombin allostery that carries over to the study of similar effects in related proteases involved in blood coagulation and the immune response.

MATERIALS AND METHODS

Site-directed mutants of human thrombin were expressed, purified, and tested for activity as described (38, 39). The equilibrium dissociation constant for Na^+ binding was determined by fluorescence titration using a FluoroMax-3 SPEX spectrophotometer, under experimental conditions of 5 mM Tris, 0.1% PEG-8000, pH 8.0 at 10 °C, I = 800 mM (8, 18). The effect of Na^+ on substrate hydrolysis was assessed from the linkage between the k_{cat}/K_m for FPR hydrolysis and [Na^+], under conditions of 5 mM Tris, 0.1% PEG-8000, pH 8.0 at 25 °C, in the presence of 200 mM NaCl or choline chloride. The value of $s = k_{cat}/K_m$, corrected for product inhibition when present (40), was calculated from the individual K_m and k_{cat} values derived from analysis of progress curves run at different substrate concentrations (from 5 up to 60 μM) and was fit according to the following equation (18, 41),

$$s = \frac{s_0 + s_1\frac{[Na^+]}{K_d}}{1 + \frac{[Na^+]}{K_d}} = s_0\frac{1 + \alpha\frac{[Na^+]}{K_d}}{1 + \frac{[Na^+]}{K_d}} \qquad \text{(Eq. 1)}$$

where s_0 and s_1 are the values of k_{cat}/K_m in the slow and fast form, respectively, and $\alpha = s_1/s_0$ is the extent of allosteric enhancement due to Na^+ binding. The value of s_0 is derived in the presence of the inert cation Ch^+ (200 mM choline chloride), whereas the value of s_1 is inferred from the value of s_0, s, and K_d. The values of K_d measured by fluorescence at 10 °C, 800 mM ionic strength, were found to be nearly identical to those measured at 25 °C, 200 mM ionic strength. This is a consequence of the compensating effects between the heat capacity change and ionic strength dependence associated with Na^+ binding to thrombin (30). The important property of Equation 1 is that it contains three independent parameters, which means that the extent of allosteric activation (α) is not necessarily linked to s_0 or to the strength of Na^+ binding (K_d). As a result, mutation of the enzyme may affect any one of these three independent parameters or any combination thereof. Mutagenesis studies can therefore identify the role of specific residues in Na^+ binding (effect on K_d) and/or allosteric transduction (effect on α).

The R77aA mutant of thrombin was used as the key reagent for all structural studies. This mutant prevents the autoproteolytic digestion of thrombin at exosite I (37) and enabled the structure of this enzyme to be obtained in the absence of any active site or exosite inhibitors for the first time (32). An important and most desirable property of the R77aA mutation is that it has no effect on the Na^+ binding properties or the catalytic activity of the enzyme (38, 39). The mutant was concentrated to 14 mg/ml in 50 mM choline chloride, 20 mM MES, pH 6.0. For crystallization with PPACK, the mutant was mixed with PPACK at a molar ratio of 1:15 and incubated at room temperature for 1 h. Crystallization was achieved at 25 °C by vapor diffusion, with each crystallization well containing 500 μl of reservoir solution. Equal volumes of the protein sample and reservoir solution (2.5 μl each) were mixed to prepare the hanging drops. Reservoir solution for the different forms were as follows: free slow form (**S**), 14% PEG-2000 monomethyl ether, 0.1 M Tris, pH 7.5; free fast form (**F**), 19% PEG-2000 monomethyl ether, 0.1 M BisTris, pH 6.6, 200 mM NaCl; PPACK-bound slow form (**SL**): 12% PEG-2000 monomethyl ether, 0.1 M Tris, pH 7.6; PPACK-bound fast form (**FL**), 14% PEG-2000 monomethyl ether, 0.1 M Tris, pH 7.6, 200 mM NaCl. Diffraction quality crystals (~0.1 × 0.1 × 0.4 mm for **S**, ~0.1 × 0.1 × 0.4 mm for **F**, ~0.1 × 0.1 × 0.9 mm for **SL**, ~0.1 × 0.1 × 0.6 mm for **FL**) were grown after 7 days. Crystals were cryoprotected in a solution similar to its reservoir solution but containing 5% additional PEG-2000 monomethyl ether and 25% glycerol prior to flash-freezing. Data were collected at the Advanced Photon Source (beamline Biocars 14-ID, Argonne National Laboratory) and processed using the HKL2000 package (42). The crystals were orthorhombic of space group $P2_12_12_1$ and contained two molecules per asymmetric unit. The A monomer of each structure was used for structural comparisons among the four crystals. Except for surface residues subject to an asymmetric crystalline environment, the differences between the A and B monomers in the asymmetric unit of each crystal were found to be negligible, including in the regions bearing the bulk of the structural changes linked to the slow → fast transition. The final refinement and model quality statistics are presented in Table I. The **S** and **F** structures were solved by molecular replacement using the coordinates of the thrombin-PPACK complex (35) and the program package CNS (43). Crystallographic refinement was carried out by simulated annealing and conjugated-gradient minimization using CNS (43). Model building was performed with the program O (44). The structures of **FL** and **SL** were solved using the same coordinates of the thrombin-PPACK complex (35) and the program package CCP4 (45). Crystallographic refinement of **FL** and **SL** was carried out by several cycles of conjugate-gradient minimization of atomic positions and temperature factor refinement in the program package CNS. Model building was performed with the program XTALVIEW (46). The autolysis loop is well defined in the **SL** structure but could not be resolved in the **FL**, **S**, and **F** structures. Water molecules were added in the final stage of the refinement process. They were subject to visual inspection to check their positioning in electron density and allowed to refine freely. Water molecules with temperature factor (B factor) higher than 80 Å^2 were excluded from subsequent refinement steps. All solvent molecules were checked with the program WASP for correct coordination and Na^+ specific valence (47). The valence for Na^+ bound to **F** and **FL** was 1.00 v.u. in both cases and the B factor was 53 (**F**) and 27 (**FL**) Å^2. No water molecule was found to have a Na^+ specific valence > 0.5 v.u. in any of the four structures analyzed. Structural comparisons were computed using LSQMAN (48). Coordinates of the structures of the R77aA thrombin mutant in the **S**, **F**, **SL**, and **FL** forms have been deposited to the Protein Data Bank (accession codes: 1SGI for **S**, 1SG8 for **F**, 1SHH for **SL**, 1SFQ for **FL**).

RESULTS

Seventy-eight residues of thrombin located in the most critical functional regions of the enzyme, *i.e.* exosite I, exosite II, the 60-loop, the specificity sites S1–S4, and the Na^+ binding site, were targeted by mutagenesis, and the Na^+ binding affinity was measured for each of them (Fig. 1). The functional epitope for Na^+ binding mapped by Ala-scanning mutagenesis

[1] The abbreviation used are: PPACK, H-D-Phe-Pro-Arg-chloromethylketone; FPR, H-D-Phe-Pro-Arg-*p*-nitroanilide; PEG, polyethylene glycol; MES, 4-morpholineethanesulfonic acid; BisTris, 2-[bis(2-hydroxyethyl)amino]-2-(hydroxymethyl)propane-1,3-diol; r.m.s., root mean square.

TABLE I
Crystallographic data on the slow and fast forms of thrombin

	S	F	SL	FL
Data collection	1SGI	1SG8	1SHH	1SFQ
Wavelength (Å)	0.9	0.9	0.9	0.9
Space group	$P2_12_12_1$	$P2_12_12_1$	$P2_12_12_1$	$P2_12_12_1$
Unit cell dimensions (Å)	a = 61.8 b = 68.1 c = 162.7	a = 59.5 b = 65.6 c = 162.4	a = 61.4 b = 68.3 c = 162.9	a = 61.3 b = 68.2 c = 162.9
Resolution range (Å)	30–2.3	30–2.3	40–1.55	40–1.9
Observations	144,752	138,252	524,286	309,158
Unique observations	27,032	27,068	94,510	53,183
Completeness	86.0 (40.2)	92.9 (70.9)	94.0 (62.9)	99.4 (96.2)
R_{sym} (%)	5.5 (17.9)	7.8 (25.7)	5.6 (35.1)	4.7 (21.5)
$I/\sigma(I)$	24.1 (5.3)	16.9 (2.6)	27.4 (2.4)	34.2 (6.5)
Refinement				
Resolution (Å)	25.0–2.3	25.0–2.3	25.0–1.55	25.0–1.9
$\|F\|/\sigma(\|F\|)$	>0	>0	>0	>0
R_{cryst}, R_{free}	0.200, 0.251	0.212, 0.234	0.195, 0.217	0.191, 0.222
Reflections (working/test)	24,288/1,787	22,836/1,724	87,597/4,608	48,669/4,448
Protein atoms	4526	4491	4652	4600
Solvent molecules	323	345	483	326
r.m.s. deviation bond lengths[a] (Å)	0.006	0.007	0.010	0.011
r.m.s. deviation angles[a] (°)	1.3	1.4	1.6	1.6
r.m.s. deviation ΔB values[a] ($Å^2$) (*m.c./s.c.*)[b]	2.6/4.0	2.6/4.0	2.1/4.0	1.8/3.0
⟨B⟩ protein, molecule A ($Å^2$)	42	50	24	29
⟨B⟩ protein, molecule B ($Å^2$)	39	49	23	30
⟨B⟩ solvent ($Å^2$)	45	51	34	36
Ramachandran plot[c]				
Most favored (%)	83.5	83.1	85.7	86.2
Additionally allowed (%)	15.5	16.7	13.6	12.8
Disallowed (%)	0.2	0.0	0.2	0.2

[a] r.m.s. deviation from ideal bond lengths and angles and r.m.s. deviation in *B* factors of bonded atoms.
[b] m.c., main chain; s.c., side chain.
[c] Calculated using PROCHCK (102).

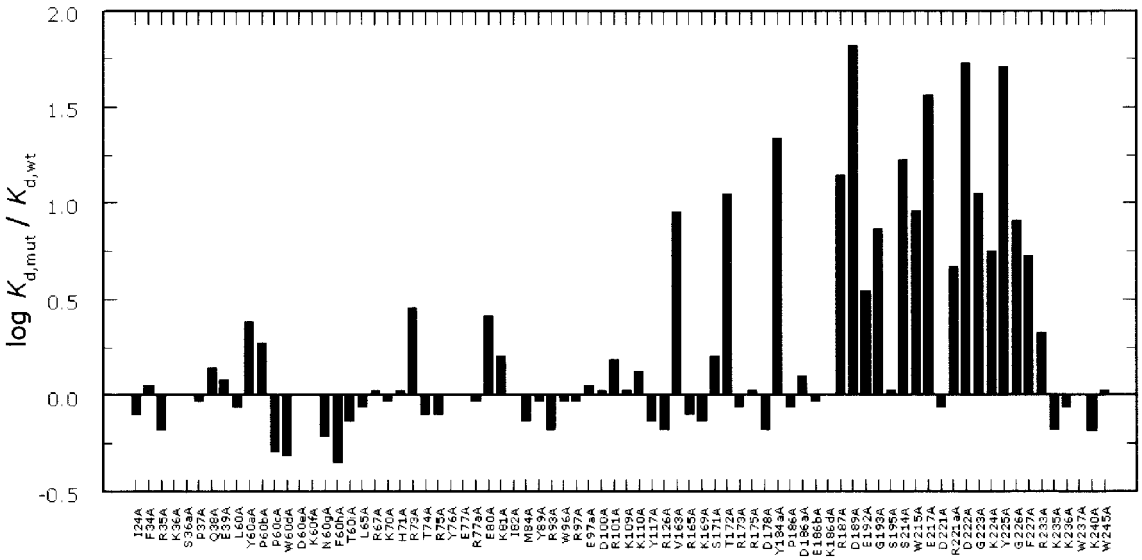

FIG. 1. **Ala-scanning mutagenesis mapping of the allosteric core of thrombin.** Shown is the change in Na^+ affinity due to mutation, expressed as log $K_{d,mut}/K_{d,wt}$, under experimental conditions of 5 mM Tris, 0.1% PEG, pH 8.0 at 10 °C, I = 800 mM. Residues of the allosteric core (Asp-189, Glu-217, Asp-222, and Tyr-225) experience a drop in Na^+ affinity >30-fold (1.5 log units). Residues Thr-172, Tyr-184a, Arg-187, Ser-214, and Gly-223 affect the Na^+ affinity >10-fold upon Ala substitution. The value of $K_{d,wt}$ is 15 ± 1 mM.

defines the "allosteric core" of residues linked to the slow → fast transition. These residues also represent prime candidates for identifying structural changes linked to Na^+ binding, although incomplete overlap often exists between functional and structural epitopes (39, 49–51).

Practically all residues of the allosteric core cluster around the Na^+ site and none of them resides in exosite I, exosite II, or the 60-loop (Fig. 2). Na^+ binding is severely compromised (>30-fold increase in K_d) upon mutation of Asp-189, Glu-217, Asp-222, and Tyr-225 that reside within 5 Å from the bound Na^+ (Fig. 3). Asp-189 fixes the orientation of one of the four water molecules ligating Na^+ and provides an important link between the Na^+ site and the P1 residue of substrate (52). Glu-217 makes polar contacts with Lys-224 and Thr-172 that help stabilize the intervening 220-loop in the Na^+ site. Mutation of Lys-224 and Thr-172 also affects Na^+ binding, although to a lesser extent compared with E217A. Notably, the naturally occurring mutant prothrombin Scranton carries the K224T substitution and is associated with a bleeding phenotype due to reduced Na^+ binding (26). The ion pair between Arg-187 and

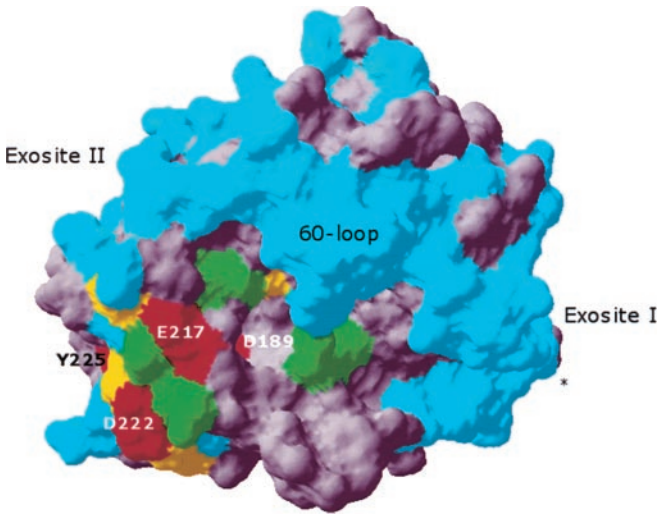

FIG. 2. **Space filling model of thrombin in the SL form depicting the structural organization of the allosteric core.** Residues affected by Ala replacement are color-coded based on the log change in the K_d for Na^+ binding (see also Fig. 1): *cyan*, ±0.5 units (3-fold); *green*, 0.5–1.0 units (3–10-fold); *yellow*, 1.0–1.5 units (10–30-fold); *red*, >1.5 units (>30-fold). Residues not subject to Ala-scanning mutagenesis are in *gray*. Note how the allosteric core (residues in *red*, marked) is confined to the region around the Na^+ binding site, nestled between the 220-loop and the 186-loop. Residues affecting Na^+ binding >10-fold (*yellow*) are in close contact with residues of the allosteric core. Exosite I, exosite II, and the 60-loop contain no residues energetically influenced by Na^+ binding. The site of mutation, R77a in exosite I, is marked by an *asterisk*.

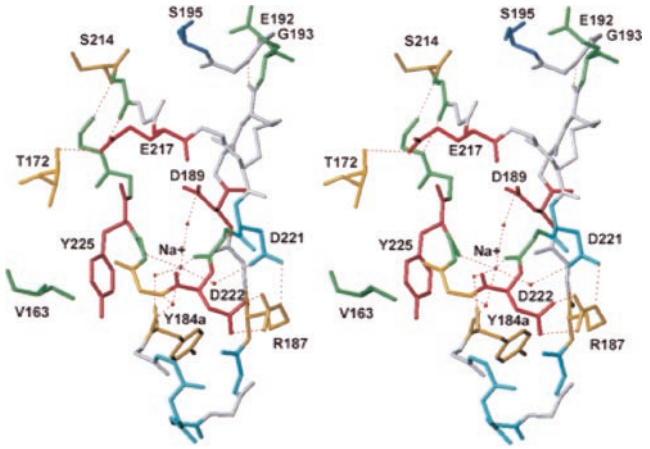

FIG. 3. **Stereo view of the molecular environment of the Na^+ binding site of thrombin showing the residues of the allosteric core (*red*).** The bound Na^+ is shown in *blue* with its coordinating water molecules (*red balls*). H-bonds are depicted as *broken lines*. Residues are color-coded as described in the legend to Fig. 2. Note the spatial proximity of the residues within the allosteric core and their close interactions with those affecting the Na^+ affinity >10-fold (*yellow*, Gly-223 is not labeled). Other residues affecting the Na^+ affinity >3-fold (*green*) or <3-fold (*cyan*) are shown as *backbone traces*, except Asp-221 that plays a key role in transducing Na^+ binding into enhanced catalytic activity, Glu-192, the active site Ser-195 and Val-163 near the side chain of Tyr-225. Residues not subject to mutagenesis are shown as *backbone traces* in *gray*.

Asp-222 latches the 186-loop onto the 220-loop to stabilize the Na^+ site and the pore of entry of the cation to its binding site (8). Mutation of Arg-187 also affects Na^+ binding, although to a lesser extent compared with D222A. The naturally occurring mutant prothrombin Greenville carries the R187Q substitution and is associated with a bleeding phenotype, again due to reduced Na^+ binding (25). Tyr-225 plays a crucial role in determining the Na^+-dependent allosteric nature of serine proteases (9) by allowing the correct orientation of the backbone O atom of residue 224 (53), which contributes directly to the coordination of Na^+. The side chain of Tyr-225 also secures the integrity of the water channel embedding the primary specificity pocket, which is required for correct substrate recognition (53).

The four residues of the allosteric core occupy crucial positions around the bound Na^+ and help maintain the integrity of the coordination shell around the bound cation. The allosteric core is assisted by another set of residues whose Ala substitution affects Na^+ binding >10-fold. These residues are Thr-172, Tyr-184a, Arg-187, Ser-214, and Gly-223. Residue 172 plays a crucial role in determining the primary specificity of trypsin and chymotrypsin (54). In thrombin, Thr-172 is oriented away from the primary specificity pocket and assumes a new role by H-bonding to Glu-217 (Fig. 3) and making contacts with Ile-174 in the aromatic S3-S4 recognition site (35). In this manner, Thr-172 links Glu-217 in the allosteric core to residues involved in substrate recognition. Tyr-184a provides an anchor to a water molecule that participates in Na^+ coordination. In the structure of thrombin bound to Rb^+ (12), and in the structure of activated protein C bound to Na^+ (17), the backbone O atom of this residue directly coordinates the cation. Arg-187 is ion-paired to Asp-222 in the allosteric core. Ser-214 controls substrate dissociation from the active site (18) and assists the catalytic triad in its function (15). Gly-223 makes an important H-bond through its backbone N atom with one of the four water molecules in the Na^+ coordination shell. Taken together, the four residues of the allosteric core (Asp-189, Glu-217, Asp-222, Tyr-225) and their five partners (Thr-172, Tyr-184a, Arg-187, Ser-214, Gly-223) form a network that links structurally and energetically the Na^+ binding site to the S3-S4 specificity pocket and the S1 specificity site.

Knowledge of the effect of Ala mutations on the energetics of Na^+ binding enables a detailed mapping of the allosteric transduction of this event into enhanced catalytic activity toward the chromogenic substrate FPR. FPR is the cleavable analog of PPACK, and its interaction with the thrombin active site (35, 53) is known to mimic that of fibrinogen (55, 56) and PAR1 (38, 57) both structurally and energetically (38). Direct measurements of s, s_0, and K_d allow determination of the values of s_1 using Equation 1. That in turn yields a molecular mapping of the effect of the mutations on FPR hydrolysis by the slow and fast forms of thrombin (Fig. 4, *bottom*) and on the parameter α in eq 1 (Fig. 4, *top*). Fig. 4 identifies residues that contribute differentially to substrate binding in the slow and fast forms. Mutations that decrease or increase significantly (>3-fold) the value of α pinpoint residues that play a predominant role in the fast or slow form, respectively. Asp-189 and Asp-221 emerge as key residues controlling substrate binding to the fast form and allosteric transduction. Asp-189 is part of the allosteric core and defines the primary specificity of the enzyme by coordinating directly the guanidinium group of Arg at P1 of substrate. Asp-221 is a crucial component of the Na^+ binding site (Fig. 3), with its side chain anchoring one of the four water molecules ligating Na^+ and also H-bonding to Asp-189. Mutation of Asp-221 does not affect Na^+ binding but almost abrogates the Na^+-induced enhancement of substrate hydrolysis. Interestingly, Asp-221 is absolutely conserved in thrombins from hagfish to human (58), lending support to the crucial role of this residue in thrombin allostery. On the other hand, Pro-60c, Ser-214, and Gly-223 facilitate substrate binding to the slow form because Ala substitution of these residues increases significantly the value of α. Pro-60c makes direct contact with substrate and defines portions of the S2 specificity pocket where the Pro residue of PPACK fits snugly. Ser-214 donates a backbone H-bond to the backbone N atom of the P1 residue of

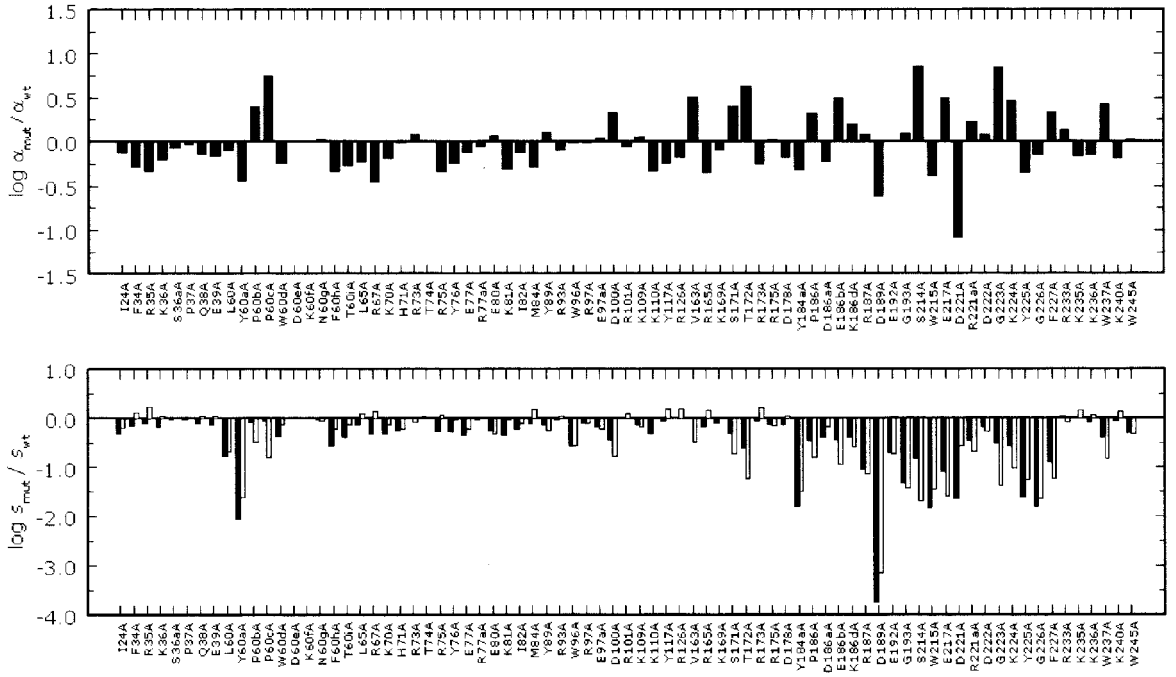

FIG. 4. **Ala-scanning mutagenesis mapping of thrombin recognition of the synthetic substrate FPR in the slow (*white bars*, s_0 values) and fast (*black bars*, s_1 values) forms.** Experimental conditions are: 5 mM Tris, 0.1% PEG, pH 8.0 at 25 °C, I = 200 mM. Also shown (*top panel*) is the effect of mutations on the allosteric transduction of Na^+ binding into enhanced catalytic activity as quantified by the parameter $\alpha = s_1/s_0$ (see Equation 1). Values in the plot are expressed as log changes relative to wild type (s_0 = 5.3 ± 0.3 μM^{-1} s^{-1}, s_1 = 95 ± 5 μM^{-1} s^{-1}, α = 18 ± 1). The plot identifies residues that control preferential substrate binding to the slow or fast form of thrombin. Residues that facilitate substrate interaction with the fast form show a significantly (>3-fold) reduced value of α upon mutation to Ala. These residues are Asp-189 and Asp-221. Residues that facilitate substrate interaction with the slow form show a significantly (>3-fold) increased value of α upon mutation to Ala. These residues are Pro-60c, Ser-214, and Gly-223.

substrate and technically defines part of the primary specificity pocket (15, 59). Gly-223 makes no contact with substrate, but its backbone N atom H-bonds to one of the four water molecules in the Na^+ coordination shell. The results reported in Fig. 4 detail how the allosteric effect of Na^+ binding on thrombin catalytic activity is distributed among residues of the protein. That information is crucial to future studies aimed at engineering Na^+ binding and enhanced catalytic activity in proteases devoid of this property.

The allosteric core defined by mutagenesis data suggests that Na^+ binding to thrombin influences residues in the immediate proximity to the cation binding site, namely Asp-189, Glu-217, Asp-222, and Tyr-225. Other residues making contacts with the ligating water molecules in the coordination shell are Tyr-184a, Asp-221, and Gly-223, and their mutation to Ala affects Na^+ binding > 10-fold (Tyr-184a, Gly-223) or affects the allosteric transduction of this event into enhanced catalytic activity (Asp-221). An obvious question arises about the structural basis of the involvement of these and other residues in thrombin allostery. The thermodynamic linkage between Na^+ and substrate binding to trombin can be formulated as shown in Scheme 1, where **S** and **F** refer to the Na^+-free (slow) and Na^+-bound (fast) forms in the free conformation (6), and L denotes substrate. Of the four intermediates in Scheme 1, only **FL** and **S** were previously solved structurally (32, 35). The structures of the **F** and **SL** intermediates are presented here for the first time, together with high resolution structures of **S** and **FL**. The structures were all obtained with the same reagent, the thrombin mutant R77aA, which retains the properties of wild type toward Na^+ binding and substrate hydrolysis (38). The new structure of **S**, solved at 2.3-Å resolution, reproduces the original observations at 2.8-Å resolution (32) and documents a slow form that is fully folded and capable of binding substrate, consistent with more than a decade of

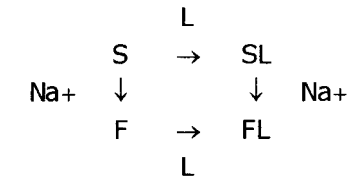

SCHEME 1

biochemical studies (6, 19, 20). The structures of the four intermediates are highly similar, with r.m.s. deviations of the Cα traces ranging from 0.38 (**F** *versus* **S**) to 0.19 (**FL** *versus* **SL**) Å. The 148-loop (or autolysis loop) is well defined only in the **SL** structure and assumes a conformation quite different from that seen in the original **FL** structure with the wild-type enzyme (35). The intrinsic and well documented flexibility of this loop, however, makes it difficult to assign a functional significance to the change. Much of the 148-loop can in fact be removed from the enzyme without significant changes in functional properties (60). A small (1 Å) upward shift is observed in the 60-loop in the structure of **S** relative to the other intermediates, but again its functional significance in the context of the Na^+-dependent allostery of thrombin is called into question by the results of Ala-scanning mutagenesis (Figs. 1 and 4). The bound PPACK and its environment in the **FL** and **SL** structures assume conformations nearly identical to those in the previously reported **FL** structure with the wild-type enzyme (35). The **SL** and **FL** structures are practically identical to each other except for the obvious absence of Na^+ in **SL**. A comparison of the *B* factor plots for these structures documents the high similarity in their conformation, whereas the **S** and **F** forms show relatively higher variability (Fig. 5). In all cases, the presence of Na^+ consistently increases the temperature factors of the structure, underscoring a higher entropy content

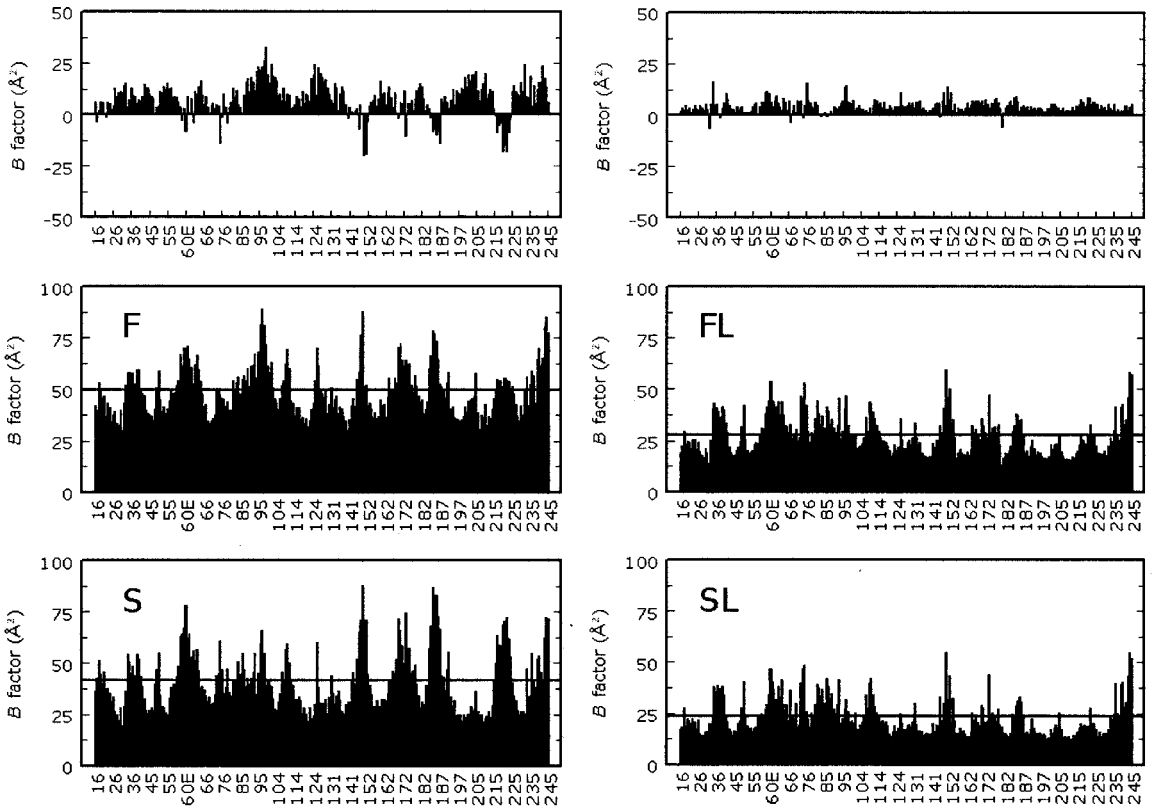

FIG. 5. **Temperature factors (*B* factors) for the structures of the four intermediates of thrombin S (free slow form), F (free fast form), SL (PPACK-bound slow form), and FL (PPACK-bound fast form).** The difference plots (fast *versus* slow) are given in the *top panels*. The plots document the intrinsically higher entropic content of the Na^+-bound forms and the substantial similarity of the PPACK-bound intermediates. The free intermediates show more variability, mostly in regions not directly involved in Na^+ or PPACK recognition. The average *B* factors for each intermediate (*continuous lines*) are: 41 ± 14 Å² (**S**), 49 ± 12 Å² (**F**), 23 ± 9 Å² (**SL**), and 28 ± 9 Å² (**FL**).

in the fast form, free or bound to PPACK. The increased *B* factors in the presence of Na^+ suggest that the increased catalytic competence of the fast form may be entropy-driven, which is consistent with kinetic data (18). The presence of PPACK forces a shift in the orientations of the side chains of Ser-195 and His-57 to allow covalent bond linkage to the inhibitor. In addition, the inhibitor causes a movement of up to 1 Å of the 191–193 strand and a reorientation of the side chain of Glu-192 (Fig. 6). The presence of PPACK has no effect on the Na^+ environment when comparing **F** with **FL** but shifts the orientation of Asp-189 when comparing **S** with **SL** (Figs. 7 and 8). More significant and informative structural changes are caused by Na^+ binding and are revealed by comparison of the free thrombin structures **S** and **F** (Figs. 8 and 9). These structures can also be discussed directly in the context of the mutagenesis studies on the allosteric core identified from measurements of Na^+ binding to the free form of the enzyme.

There are five main structural differences between the slow (**S**) and fast (**F**) forms of thrombin: 1) the Arg-187:Asp-222 ion pair, 2) the orientation of Asp-189 in the primary specificity pocket, 3) the orientation of Glu-192 at the entrance of the active site, 4) the orientation of the catalytic Ser-195, and 5) the architecture of the water network spanning >20 Å from the Na^+ site to the active site. These differences will be discussed in order.

The Arg-187:Asp-222 ion pair connects the 220- and 186-loops that define the Na^+ site. Asp-222 belongs to the allosteric core, and the mutant D222A has drastically impaired Na^+ binding, a property mirrored to smaller extent by the R187A mutant (Fig. 1). In the fast form (**F**) the guanidinium N atoms of Arg-187 are 2.7 and 3.1 Å from the carboxylate O atoms of Asp-222 (Figs. 8 and 9), with similar distances in the PPACK-bound forms (**FL** and **SL**). In the slow form (**S**), these distances become 3.3 Å and 4.8 Å respectively (Figs. 8 and 9). There is also a rotation of the plane of the carboxylate of Asp-222 relative to the plane of the guanidinium group of Arg-187 in the slow form, bringing the two groups further apart. Breakage of the ion pair was already observed in the low resolution structure of the slow form (32) and is consistent with the mutagenesis data supporting a slow form type of behavior for the R187A and D222A mutants (Fig. 4). Importantly, the breakage causes a shift in the backbone O atom of Arg-221a that directly coordinates Na^+ in the fast form and moves it into an orientation that is incompatible with Na^+ binding.

Asp-189 in the fast form (**F**) is optimally oriented for electrostatic coupling with the P1 Arg residue of substrate and has the same conformation as in the PPACK-inhibited slow (**SL**) or fast (**FL**) forms. In the slow form (**S**), however, the carboxylate of Asp-189 experiences a 30° rotation that moves the Oδ1 atom up to 1.1 Å away from its optimal coupling with the guanidinium group of Arg at the P1 position of substrate (Figs. 8 and 9). The rearrangement of Asp-189 upon Na^+ binding, first detected in the low resolution structure of the slow form (32), is an important factor in the enhancement of substrate specificity, which is almost abrogated with the D189A mutation (Fig. 4). The structure of the slow form supports a key role for Asp-189 in both Na^+ coordination and allosteric transduction of Na^+ binding into enhanced catalytic activity (52), consistent with the results of our mutagenesis data.

The entire strand from 191 to 193 does not change appreciably in the slow → fast transition but experiences a 1-Å upward shift when PPACK is bound to the active site in either form (Fig. 6). The movement, first emerged from the low resolution structure of the slow form (32), is therefore induced by inhibitor

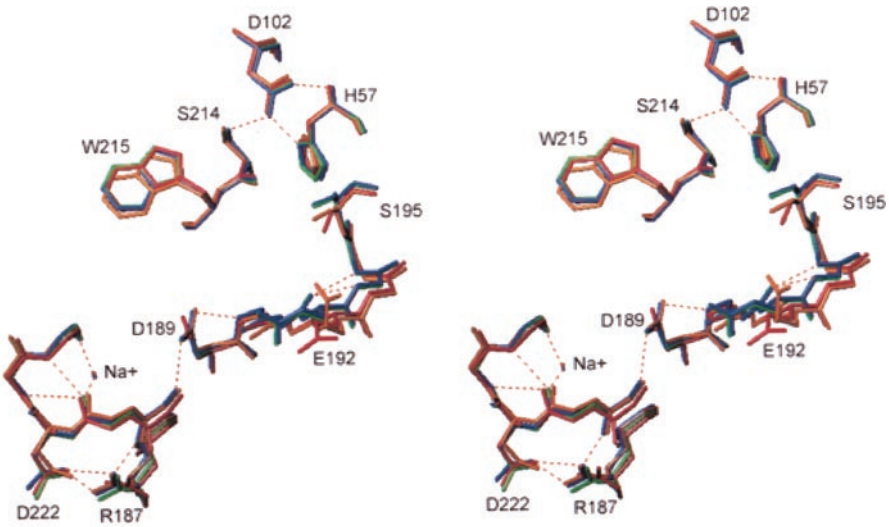

FIG. 6. **Stereo view of the structural changes induced by Na^+ and/or PPACK binding to thrombin.** Structures depict **F** (free fast form, *gold*), **S** (free slow form, *red*), **FL** (PPACK-bound fast form, *blue*), and **SL** (PPACK-bound slow form, *green*). The bound PPACK in the **SL** and **FL** structures was omitted to expose the changes at the level of Ser-195. Shown are the changes in the Arg-221a backbone (**S**), the breakage of the Arg-187:Asp-222 ion pair (**S**), the reorientation of Asp-189 (**S**), the upward shift of the 191–193 strand (**SL** and **FL**), the reorientation of Glu-192 (**S** and **F**), and the shift in the position of the Oγ atom of Ser-195 (**S** and **F**). H-bonds are shown by *broken lines* and refer to the **FL** structure.

binding to the active site and not by Na^+ binding. A similar shift of about 1 Å is documented in the backbone of the 60-loop in the slow form, causing a modest rearrangement of Trp-60d. The changes around Trp-60d, however, are not linked energetically to Na^+ binding (Fig. 1) or allosteric transduction (Fig. 4). None of the residues in the 60-loop is involved in promoting binding to the fast form. In fact, Pro-60c acts to counter the allosteric enhancement induced by Na^+ binding and promotes substrate interaction with the slow form (Fig. 4). The side chain of residue Glu-192 shows flexibility in the slow and fast forms (Figs. 8 and 9), which is tempered by binding of PPACK to the active site (Fig. 6). This is consistent with previous structural data of the fast form inhibited at exosite I with hirugen and with the active site free (36). Notably, the movement of Glu-192 in the slow form relative to the fast form brings the carboxylate away from the active site region and confirms previous findings from the low resolution structure of the slow form (32). This movement minimizes the potential electrostatic clash with the P3 and P3′ acidic residues of protein C and explains why the slow form of thrombin retains high activity toward the anticoagulant substrate protein C (20, 61, 62).

The catalytic Ser-195 retains signature of important conformational changes first emerged from the low resolution structure of the slow form (32). The side chain of Ser-195 rotates about 35° in the slow form relative to the fast form and breaks the H-bond with the catalytic His-57, which also shifts slightly away from Ser-195. Because of the neutral pH used in growing the crystals, this H-bond is expected to be intact (15). Indeed, the H-bond is present in the fast form inhibited with hirugen and with the active site free (36). Hence, the changes around Ser-195 observed in the slow form (**S**) relative to the fast form (**F**) are due to the absence of Na^+. The conformation of Ser-195 in the slow form likely reduces substrate recognition and especially the k_{cat}. The energy cost of realigning Ser-195 for H-bonding with His-57 contributes to the lower specificity constant of the slow form compared with the fast form. It should be pointed out that the conformation of Ser-195 in the fast form (**F**) is also not optimal for substrate recognition and is intermediate to that of the slow form and the PPACK-bound forms (Fig. 6). These changes lend support to the idea that the nucleophile of Ser-195 can be repositioned within the active site and that Na^+, and possibly other cofactors of thrombin like thrombomodulin, may take advantage of this flexibility to modulate the enzyme activity. The change in the position of Ser-195 is not linked energetically to Na^+ binding (Fig. 1). Most likely, the change is responsible for transducing Na^+ binding into enhanced catalytic activity, as for residue Asp-221, but the lack of activity of the S195A mutant makes conclusive demonstration of this point difficult.

The structural changes of the slow → fast transition of thrombin do not involve Glu-217 and Tyr-225 in the allosteric core identified by mutagenesis. These residues appear in the same conformation in the four intermediates of thrombin free/bound to Na^+ and/or PPACK. Likewise, there are no significant changes around Asp-221, which plays a dominant role in the allosteric enhancement of catalytic activity, or around Thr-172 and Ser-214. The lack of structural changes at the level of residues energetically involved in thrombin allostery may be subject to diverse interpretations. The changes undergone by these residues may be too small to detect crystallographically, or the conditions used in our crystal studies are not optimal to identify them. A significant structural change between the slow and fast forms, however, does exist and provides evidence of long range communication between the Na^+ site and the active site. Previous studies of thrombin in the fast form have pointed out a network of water molecules that embeds the Na^+ site, the primary specificity site, and the active site (16, 63). This network was first discovered in the structure of thrombin inhibited at exosite I with hirugen and with the active site free (36). The presence of PPACK, or other active site inhibitors of thrombin, eliminates most of the bound water molecules in the region and obscures the role that solvent plays in thrombin allostery. In the fast form, there is a network of eleven water molecules that connect through H-bonds the bound Na^+ to the Oγ atom of Ser-195, located >15 Å away (Figs. 8 and 9). These solvent molecules act as links between the strands 215–219, 225–227, and 191–193, which define the Na^+ site and the walls of the primary specificity pocket, and fine tune the function of these strands in controlling substrate docking into the active site. In the slow form, only seven water molecules occupy positions in the network equivalent to those seen in the fast form and the connectivity is radically altered.

DISCUSSION

The results presented in this investigation of Na^+ binding to thrombin identify structural determinants responsible for the Na^+-dependent enhancement of catalytic activity. The residues energetically linked to Na^+ binding concentrate around the Na^+ site and connect up with residues involved in substrate binding and catalysis via H-bonds and water mediated contacts. The structural changes underlying Na^+ binding are small but appear at critical locations within the protein. These results are in line with the effects documented in other allosteric systems. Practically all monovalent cation-activated en-

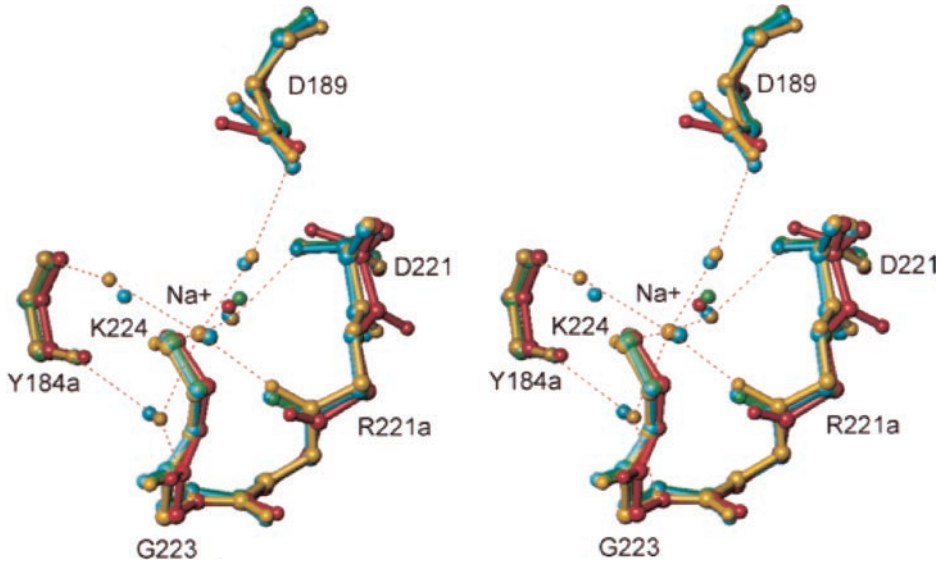

FIG. 7. **Stereo view of the Na^+ binding environment in the structures of F (free fast form, *gold*), S (free slow form, *red*), FL (PPACK-bound fast form, *blue*), and SL (PPACK-bound slow form, *green*).** Shown are all atoms within 3 Å of the bound Na^+ in the **F** structure, in addition to the side chains of Asp-189 and Asp-221. Note the similarity of the Na^+ coordination shell between **F** and **FL**; the bound Na^+ is coordinated octahedrally by the backbone O atoms of Lys-224 and Arg-221a and by four buried water molecules that H-bond to (clockwise) Asp-189, Asp-221, Gly-223, and Tyr-184a. Only some of these water molecules are replaced in the absence of Na^+ (**S** and **SL**). Note the rearrangement of the side chain of Asp-189 in the **S** structure and the significant shift in the backbone O atom of Arg-221a that assumes a position incompatible with Na^+ coordination. H-bonds are shown by *broken lines* and refer to the **F** structure.

zymes investigated structurally to date (64–69) show conformational changes induced by cation binding that are small but of extreme functional relevance. In the case of dialkylglycine decarboxilase, for example, the effect of Na^+ on the enzyme is mediated by the reorientation of a Ser residue near the active site induced by cation binding (65, 66). In the case of Trp synthase, binding of Na^+ triggers small local and long range changes in the quaternary structure (69). In transmembrane receptors, subtle conformational changes as small as 1 Å are transmitted from ligand binding sites to effector sites over distances greater than 100 Å using H-bonding networks (70, 71).

The highly conserved fold of serine proteases has fostered the notion that these enzymes are quite rigid and that even drastic perturbations of their functional properties are difficult to pinpoint structurally (15, 59). There is copious experimental support to this view. The strength of substrate binding to trypsin is affected significantly by small shifts in the backbone of residues Ser-214 and Gly-216 (72, 73). In the case of thrombin, the mutation Y225I impairs substrate recognition up to five orders of magnitude, but the structure of Y225I bound to PPACK is practically identical to that of wild type (53). Likewise, binding of thrombomodulin to thrombin causes little structural changes (74), although the interaction increases the specificity toward protein C >1,000-fold (75). However, examples of significant conformational changes do exist in serine proteases. Staphylocoagulase induces structural transitions of prothrombin that result in an active conformation of the zymogen (76). The E192Q mutant of thrombin bound to the trypsin inhibitor BPTI displays a drastic change in the conformation of the otherwise rigid 60-loop (77). In the case of coagulation factor VII, binding of tissue factor causes large structural rearrangements that are consistent with the large shift in catalytic activity (78, 79). These findings are not necessarily conflicting. Proteins often overcome large energetic barriers with subtle conformational transitions that are too small to detect crystallographically. Equally often, proteins explore shallow energetic landscapes with large conformational transitions (80). Furthermore, the lattice constraints in a crystal structure can easily abrogate subtle conformational rearrangements or can amplify them into incarnations that are artifactual and never favored energetically in solution. It is therefore quite important that the results of structural studies on allosteric mechanisms are informed by and consistent with the information derived from kinetic, thermodynamic, and site-directed mutagenesis studies. This ensures identification of those structural changes that are energetically significant and those significant energetic changes that have a structural counterpart.

The structural changes documented in this study of the four possible intermediates free/bound to Na^+ and/or PPACK support the contention that thrombin function and regulation are not mediated by large scale structural transitions. In the absence of PPACK, the Na^+-induced changes in thrombin structure are revealed most eloquently. The slow → fast transition causes: 1) formation of the ion pair between Arg-187 and Asp-222 that stabilizes the 220-loop and the 186-loop and realigns the backbone O atom of R221a for Na^+ coordination, 2) shift in the side chain of Asp-189 for optimal electrostatic coupling with the guanidinium group of the P1 Arg residue of substrate, 3) shift in the side chain of Glu-192 for optimal anchoring of the crucial water molecule that connects the water network to Ser-195, and 4) shift in the side chain of Ser-195 for optimal nucleophilic attack to the incoming substrate. These changes produce a conformation more prone to bind and catalyze hydrolysis of substrates like FPR, which is a good model for fibrinogen and PAR1 (38). Consequently, the slow → fast transition optimizes thrombin for its procoagulant, prothrombotic, and signaling functions (19, 20, 81). The orientation of Glu-192 in the slow form, however, compensates for the deleterious changes around Asp-189 and Ser-195 and reduces the electrostatic clash with the acidic residues at position P3 and P3′ of protein C. That results in a conformation that retains activity toward protein C and explains the intrinsic anticoagulant nature of the slow form (19, 20, 81). The fast form of thrombin cleaves fibrinogen and PAR1 with specificity constants that are, respectively, 170 and 260-fold higher than that of protein C (81). In the slow form, however, these ratios become 4.7- and 4.4-fold, respectively (81), due to an exclusive drop of the rates of cleavage of fibrinogen and PAR1 below physiologically acceptable levels. The slow form is therefore anticoagulant be-

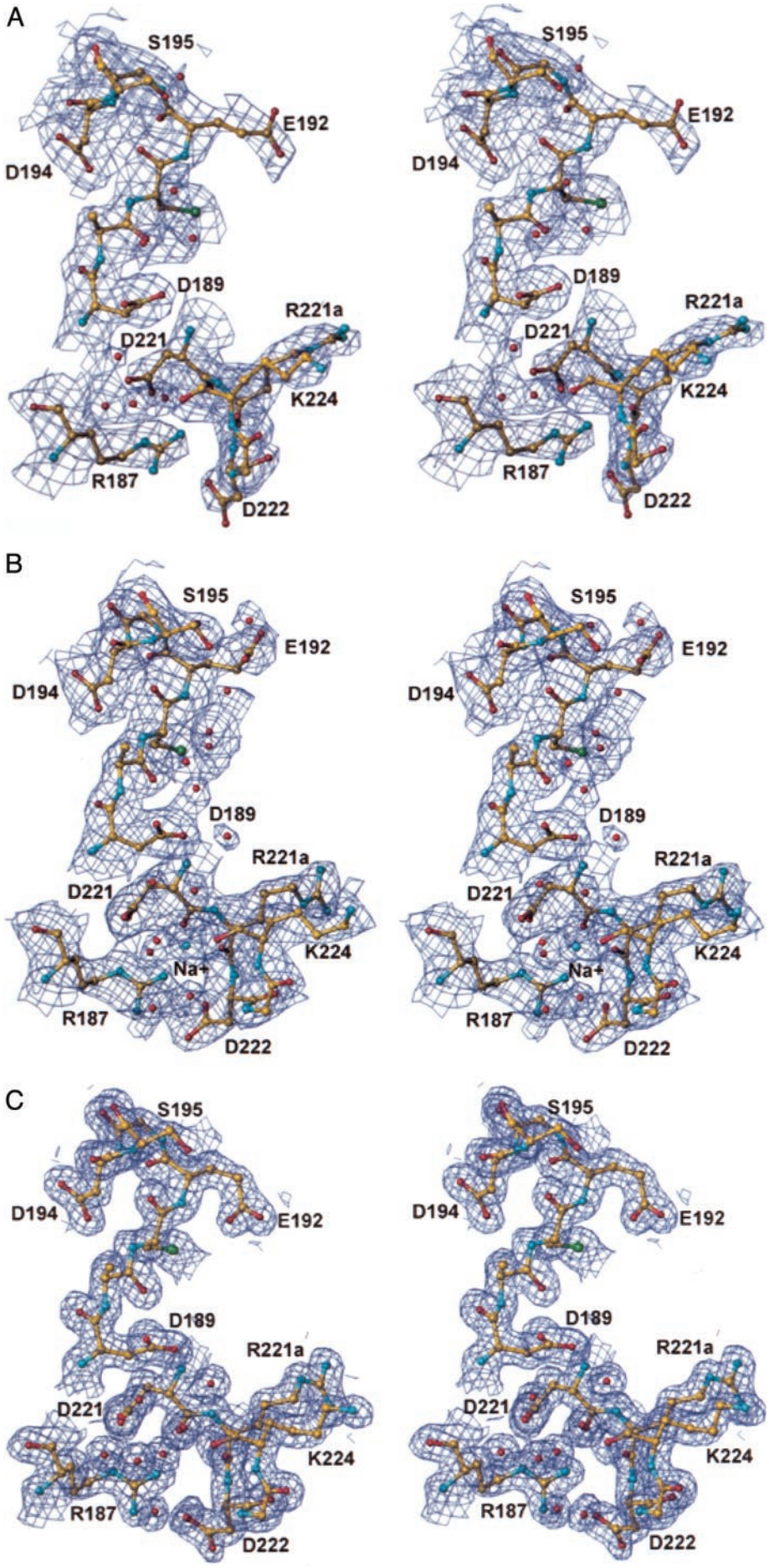

FIG. 8. **Stereo view of the electron density maps of the S (*A*), F (*B*), SL (*C*), and FL (*D*) intermediates of thrombin in the regions bearing the most significant structural transitions.** Residues are rendered in CPK. The bound Na^+ is rendered as a *cyan ball*. Shown are the 221–224 loop region and the 187–195 domain. Note how Asp-222 and Arg-187 have joined densities in the **F** form, indicative of ion pair interaction, but not in the **S** form. Also notable are the reorientation of Asp-189 and Glu-192 in the **S** form, as well as the shift in the position of Ser-195. Other changes observed in the slow → fast transition involve the network of water molecules (*red balls*) embedding the Na^+ site, the S1 pocket, and the active site region. In the fast form, this network is well organized and contains 11 water molecules. In the slow form, the water molecules are reduced to seven, and the long range connectivity of the network is lost (see also Fig. 9). The $2F_o - F_c$ electron density maps are contoured at 0.7 σ for **S** and **F** and at 1.0 σ for **SL** and **FL**.

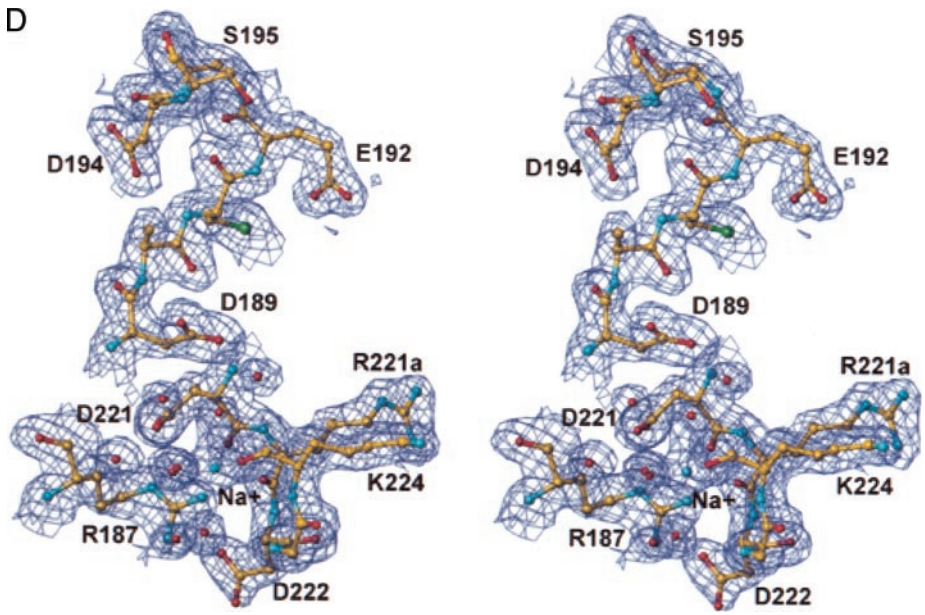

FIG. 8—*continued*

cause it retains normal (or slightly higher than normal) activity toward protein C, but it is unable to promote a physiologically acceptable cleavage of fibrinogen or PAR1. This explains why genetic defects leading to impaired Na^+ binding, such as prothrombin Frankfurt (23), Salakta (24), Greenville (25), and Scranton (26), are associated with bleeding phenotypes. Furthermore, every anticoagulant thrombin mutant reported to date has been shown to be defective for Na^+ binding (82–84). The structural results presented here provide a sound molecular interpretation of the anticoagulant properties of the slow form of thrombin.

Comparison of the allosteric core defined by Ala scanning mutagenesis and the structural changes between the slow and fast forms reveal the connection between functional and structural determinants of Na^+ recognition. Functional and structural epitopes often overlap, but notable exceptions have been reported in the literature (49–51, 85). Functional epitopes tend to be smaller than their structural counterparts and typically host residues that are tightly coupled in the recognition process (39, 50, 86). In the case of Na^+ binding to thrombin, on the other hand, the functional epitope defined by the allosteric core is significantly more extended than the small Na^+ cage documented by the crystal structure. Breakage of the Arg-187:Asp-222 ion pair in the slow form is consistent with the observation that the R187A and D222A mutants have compromised Na^+ binding. Likewise, weakening of Na^+ binding in the D189A mutant agrees well with the critical anchoring role of this residue in the Na^+ coordination shell. The functional role of other residues in the allosteric core, however, is not translated into significant structural changes. For example, mutations of Ser-214, Thr-172, Gly-223, and Tyr-184a have a significant effect on Na^+ binding, but no structural changes are detected around these residues in the slow → fast transition. It is possible that our structural results provide only a partial picture of the allosteric transition trigerred by Na^+ binding, which may be revealed fully by future structural analysis. Alternatively, the functional role of other residues in the allosteric core may not be linked to structural transitions that can be detected by x-ray crystallography.

A crucial difference between the two allosteric forms of thrombin resides in the architecture of the water network embedding the Na^+ site, the primary specificity pocket and the active site region. The role of this network is to provide the connectivity among residues distant in space, which is the hallmark of allosteric transitions. The network links the bound Na^+ to Ser-195 located >15 Å away, using the side chains of Asp-189 and Glu-192 as intermediate relays. Changes in the ordering, position, and number of these buried water molecules provide a structural explanation for the unusually large change in heat capacity observed upon Na^+ binding to thrombin (8, 30, 31). The change is the result of the formation of water binding sites connecting strands and loops of the Na^+ site by analogy to what is observed when water molecules are buried at the Trp repressor-operator interface (87). The conspicuous network of water molecules connecting the primary specificity pocket of serine proteases to the active site region has been recognized in previous studies (16, 63, 88, 89). Comparison of this network with the position of bound substrate in the active site shows how the H-bonding infrastructure of the water molecules is replaced by atoms in the P1 residue of substrate for optimal docking into the primary specificity pocket (36). Indeed, the architecture of the water network has offered precious insights in drug design (88). The data presented in this study offer a new paradigm that adds to the important role of the water network in the active site region of trypsin-like proteases. The allosteric properties of thrombin seem to depend on the structure of this water network in a decisive manner. All residues involved energetically in Na^+ binding and the allosteric transduction of this event into enhanced catalytic activity are in direct contact with water molecules in the network. The network provides the long range connectivity needed to allosterically communicate information from the Na^+ site to the active site Ser-195 and to residues involved in substrate recognition, like Asp-189 and Glu-192. It is possible that the network of water molecules may be responsible for other allosteric effects of thrombin triggered by binding to exosite I (33, 90) or exosite II (91, 92). The effect of thrombomodulin on thrombin (75) is known to involve Glu-192 (93), and the structure of **F** supports a major role for this residue in the organization of the architecture of the water network near Ser-195. The role of water in allosteric transitions of proteins and molecular recognition has been documented in several systems (87, 94, 95). The structural similarity of thrombin and other proteases involved in blood clotting and the immune response, which are also sensitive to Na^+ activation (9), suggests that serine proteases exploit water exchange in their allosteric function, a hypothesis that should be given careful consideration in future studies of these important enzymes.

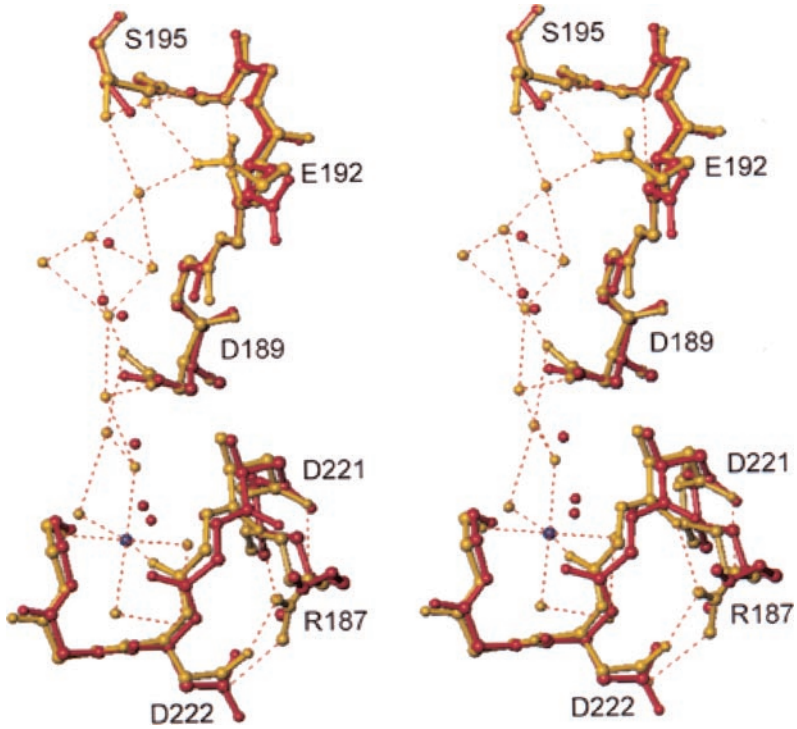

FIG. 9. **Stereo view of the structural changes induced by the slow → fast transition of thrombin depicted by the structures of F (free fast form, *gold*) and S (free slow form, *red*).** Shown are the main changes induced by Na^+ (*blue ball*) release: the breakage of the Arg-187:Asp-222 ion pair causing a shift in the backbone O atom of Arg-221a (see also Figs. 7 and 8), the reorientation of Asp-189, the shift of the side chain of Glu-192 that moves away from the active site entrance, and the shift in the position of the Oγ atom of Ser-195. These changes explain the reduced catalytic activity of the slow form toward substrate. Also shown are the changes caused by the slow → fast transition in the water network connecting the Na^+ site to the active site Ser-195. The water molecules in the fast form (*gold balls*) are well organized in a network that connects the bound Na^+ to the side chain of Asp-189 and continue on to reach the Oγ atom of Ser-195. A critical link in the network is provided by water molecule w915 that H-bonds to Ser-195 and Glu-192. This water molecule is removed in the slow form, possibly because of the reorientation of Glu-192. The connectivity of water molecules in the slow form (*red balls*) is further compromised by the lack of Na^+ and proper anchoring of the side chain of Asp-189. H-bonds are shown by *broken lines* and refer to the **F** structure. The changes in the network between the slow and fast forms help explain the large heat capacity change linked to Na^+ binding. Temperature factors of the water molecules average 52 ± 11 Å^2 in the **S** form (ranging from 39 to 72 Å^2) and 53 ± 11 Å^2 in the **F** form (ranging from 38 to 77 Å^2). The range of *B* factors (slow form/fast form) for the atoms of some critical residues shown are: Arg-187 (52–75 Å^2/46–58 Å^2), Asp-189 (36–58 Å^2/46–51 Å^2), Ser-195 (26–42 Å^2/32–47 Å^2), Glu-192 (38–75 Å^2/44–78 Å^2), Asp-221 (59–74 Å^2/41–54 Å^2), and Asp-222 (62–79 Å^2/51–63 Å^2).

A recent structure of the thrombin mutant S195A has documented a rearrangement of the side chain of Trp-60d that occludes the active site (96). The movement, along with other changes around residue Trp-215, has been invoked as an explanation of the allosteric transition of thrombin from the fast form, where the active site is fully accessible, to the slow form, where the active site is blocked. We are doubtful that this structure portrays the slow form for two reasons. First, the structure has Na^+ bound to its site, which contradicts the very definition of the slow form (6). Second, occlusion of the active site is inconsistent with the slow form displaying lower, but finite, specificity toward substrate compared with the fast form (6, 33, 81). Equally problematic is the interpretation of the recent structure of the thrombin mutant E217K (97) as portraying key properties of the slow form. This mutant shows occlusion of the active site region, which is merely a consequence of the drastic charge reversal at residue 217. Because the catalytic properties of the E217K mutant are impaired well beyond those of the slow form of wild-type thrombin, this mutant provides neither a functional nor a structural mimic of the slow form. The recent proposal that the slow form of thrombin is an inactive conformer (96, 97) has no experimental support. Data published more than 20 years ago, before the effect of Na^+ on thrombin was discovered and characterized, demonstrated that thrombin is active even under conditions of zero ionic strength (98). The proposal that occlusion of the active site in the slow form is removed by induced-fit transitions triggered by substrate binding (96) is inconsistent with the similarity of activation energies for substrate binding in the slow and fast forms (18) and with the lack of a significant energy barrier for fibrinogen or fibrin binding to thrombin in either the fast or slow form (99). Even more puzzling is to reconcile how a slow form with its active site occluded by Trp-60d could activate protein C, in the presence or absence of thrombomodulin, at a rate comparable with that of the fast form (20, 61, 62). The conformation of Trp-60d reported in the recent structure of the S195A mutant of thrombin (96) is an artifact of crystallization conditions due to the collapse of the indole ring into the active site turned more hydrophobic upon the S195A substitution. No such changes at the level of Trp-60d or Trp-215 are observed in other published structures of the S195A mutant of thrombin (100) or in structures of the S195A mutant obtained in the presence or absence of Na^+.[2] Likewise, early reports of a key role of Trp-60d in thrombin allostery based on the properties of the W60dS mutant (101) are to be considered artifactual, due to the drastic change in polarity introduced by the mutation. The Ala-scanning mutagenesis data presented here (Figs. 1 and 4) demonstrate conclusively that Trp-60d and the entire 60-loop play no significant role in the Na^+-dependent thrombin allostery.

REFERENCES

1. Mann, K. G. (2003) *Chest* **124,** 4S–10S
2. Mann, K. G., Butenas, S., and Brummel, K. (2003) *Arterioscler. Thromb.*

[2] A. Tulinsky and E. Di Cera, manuscript in preparation.

Vasc. Biol. **23,** 17–25
3. Sambrano, G. R., Weiss, E. J., Zheng, Y. W., Huang, W., and Coughlin, S. R. (2001) *Nature* **413,** 74–78
4. Coughlin, S. R. (2000) *Nature* **407,** 258–264
5. Brass, L. F. (2003) *Chest* **124,** 18S–25S
6. Wells, C. M., and Di Cera, E. (1992) *Biochemistry* **31,** 11721–11730
7. Suelter, C. H. (1970) *Science* **168,** 789–795
8. Prasad, S., Wright, K. J., Roy, D. B., Bush, L. A., Cantwell, A. M., and Di Cera, E. (2003) *Proc. Natl. Acad. Sci. U. S. A.* **100,** 13785–13790
9. Dang, Q. D., and Di Cera, E. (1996) *Proc. Natl. Acad. Sci. U. S. A.* **93,** 10653–10656
10. Krem, M. M., and Di Cera, E. (2001) *EMBO J.* **20,** 3036–3045
11. Krem, M. M., and Di Cera, E. (2002) *Trends Biochem. Sci.* **27,** 67–74
12. Di Cera, E., Guinto, E. R., Vindigni, A., Dang, Q. D., Ayala, Y. M., Wuyi, M., and Tulinsky, A. (1995) *J. Biol. Chem.* **270,** 22089–22092
13. Perona, J. J., and Craik, C. S. (1997) *J. Biol. Chem.* **272,** 29987–29990
14. Perona, J. J., Hedstrom, L., Rutter, W. J., and Fletterick, R. J. (1995) *Biochemistry* **34,** 1489–1499
15. Hedstrom, L. (2002) *Chem. Rev.* **102,** 4501–4524
16. Zhang, E., and Tulinsky, A. (1997) *Biophys. Chem.* **63,** 185–200
17. Schmidt, A. E., Padmanabhan, K., Underwood, M. C., Bode, W., Mather, T., and Bajaj, S. P. (2002) *J. Biol. Chem.* **277,** 28987–28995
18. Krem, M. M., Prasad, S., and Di Cera, E. (2002) *J. Biol. Chem.* **277,** 40260–40264
19. Di Cera, E. (2003) *Chest* **124,** 11S–17S
20. Dang, O. D., Vindigni, A., and Di Cera, E. (1995) *Proc. Natl. Acad. Sci. U. S. A.* **92,** 5977–5981
21. Rezaie, A. R., and He, X. (2000) *Biochemistry* **39,** 1817–1825
22. Camire, R. M. (2002) *J. Biol. Chem.* **277,** 37863–37870
23. Degen, S. J., McDowell, S. A., Sparks, L. M., and Scharrer, I. (1995) *Thromb. Haemostasis* **73,** 203–209
24. Miyata, T., Aruga, R., Umeyama, H., Bezeaud, A., Guillin, M. C., and Iwanaga, S. (1992) *Biochemistry* **31,** 7457–7462
25. Henriksen, R. A., Dunham, C. K., Miller, L. D., Casey, J. T., Menke, J. B., Knupp, C. L., and Usala, S. J. (1998) *Blood* **91,** 2026–2031
26. Sun, W. Y., Smirnow, D., Jenkins, M. L., and Degen, S. J. (2001) *Thromb. Haemostasis* **85,** 651–654
27. Adrogue, H. J., and Madias, N. E. (2000) *N. Engl. J. Med.* **342,** 1493–1499
28. Adrogue, H. J., and Madias, N. E. (2000) *N. Engl. J. Med.* **342,** 1581–1589
29. Owen, W. G., Bichler, J., Ericson, D., and Wysokinski, W. (1995) *Biochemistry* **34,** 9277–9281
30. Guinto, E. R., and Di Cera, E. (1996) *Biochemistry* **35,** 8800–8804
31. Griffon, N., and Di Stasio, E. (2001) *Biophys. Chem.* **90,** 89–96
32. Pineda, A. O., Savvides, S. N., Waksman, G., and Di Cera, E. (2002) *J. Biol. Chem.* **277,** 40177–40180
33. Ayala, Y., and Di Cera, E. (1994) *J. Mol. Biol.* **235,** 733–746
34. Lai, M. T., Di Cera, E., and Shafer, J. A. (1997) *J. Biol. Chem.* **272,** 30275–30282
35. Bode, W., Turk, D., and Karshikov, A. (1992) *Protein Sci.* **1,** 426–471
36. Vijayalakshmi, J., Padmanabhan, K. P., Mann, K. G., and Tulinsky, A. (1994) *Protein Sci.* **3,** 2254–2271
37. Hofsteenge, J., Braun, P. J., and Stone, S. R. (1988) *Biochemistry* **27,** 2144–2151
38. Ayala, Y. M., Cantwell, A. M., Rose, T., Bush, L. A., Arosio, D., and Di Cera, E. (2001) *Proteins* **45,** 107–116
39. Pineda, A. O., Cantwell, A. M., Bush, L. A., Rose, T., and Di Cera, E. (2002) *J. Biol. Chem.* **277,** 32015–32019
40. Krem, M. M., and Di Cera, E. (2003) *Biophys. Chem.* **100,** 315–323
41. Di Cera, E., Hopfner, K. P., and Dang, Q. D. (1996) *Biophys. J.* **70,** 174–181
42. Otwinowski, Z., and Minor, W. (1997) *Methods Enzymol.* **276,** 307–326
43. Brunger, A. T., Adams, P. D., Clore, G. M., DeLano, W. L., Gros, P., Grosse-Kunstleve, R. W., Jiang, J. S., Kuszewski, J., Nilges, M., Pannu, N. S., Read, R. J., Rice, L. M., Simonson, T., and Warren, G. L. (1998) *Acta Crystallogr. Sect. D Biol. Crystallogr.* **54,** 905–921
44. Jones, T. A., Zou, J. Y., Cowan, S. W., and Kjeldgaard. (1991) *Acta Crystallogr. Sect. A* **47,** 110–119
45. Bailey, S. (1994) *Acta Crystallogr. Sect. D Biol. Crystallogr.* **50,** 760–763
46. McRee, D. E. (1999) *J. Struct. Biol.* **125,** 156–165
47. Nayal, M., and Di Cera, E. (1996) *J. Mol. Biol.* **256,** 228–234
48. Kleywegt, G. J. (1999) *Acta Crystallogr. Sect. D Biol. Crystallogr.* **55,** 1878–1884
49. Greenspan, N. S., and Di Cera, E. (1999) *Nat. Biotechnol.* **17,** 936–937
50. Clackson, T., and Wells, J. A. (1995) *Science* **267,** 383–386
51. Schreiber, G., and Fersht, A. R. (1995) *J. Mol. Biol.* **248,** 478–486
52. Prasad, S., Cantwell, A. M., Bush, L. A., Shih, P., Xu, H., and Di Cera, E. (2004) *J. Biol. Chem.* **279,** 10103–10108
53. Guinto, E. R., Caccia, S., Rose, T., Futterer, K., Waksman, G., and Di Cera, E. (1999) *Proc. Natl. Acad. Sci. U. S. A.* **96,** 1852–1857
54. Hedstrom, L., Perona, J. J., and Rutter, W. J. (1994) *Biochemistry* **33,** 8757–8763
55. Stubbs, M. T., Oschkinat, H., Mayr, I., Huber, R., Angliker, H., Stone, S. R., and Bode, W. (1992) *Eur. J. Biochem.* **206,** 187–195
56. Rose, T., and Di Cera, E. (2002) *J. Biol. Chem.* **277,** 18875–18880
57. Mathews, I. I., Padmanabhan, K. P., Ganesh, V., Tulinsky, A., Ishii, M., Chen, J., Turck, C. W., Coughlin, S. R., and Fenton, J. W., II (1994) *Biochemistry* **33,** 3266–3279
58. Banfield, D. K., and MacGillivray, R. T. (1992) *Proc. Natl. Acad. Sci. U. S. A.* **89,** 2779–2783
59. Perona, J. J., and Craik, C. S. (1995) *Protein Sci.* **4,** 337–360
60. Dang, Q. D., Sabetta, M., and Di Cera, E. (1997) *J. Biol. Chem.* **272,** 19649–19651
61. Berg, D. T., Wiley, M. R., and Grinnell, B. W. (1996) *Science* **273,** 1389–1391
62. Rezaie, A. R., and Olson, S. T. (1997) *Biochemistry* **36,** 1026–1033
63. Krem, M. M., and Di Cera, E. (1998) *Proteins* **30,** 34–42
64. Larsen, T. M., Laughlin, L. T., Holden, H. M., Rayment, I., and Reed, G. H. (1994) *Biochemistry* **33,** 6301–6309
65. Toney, M. D., Hohenester, E., Cowan, S. W., and Jansonius, J. N. (1993) *Science* **261,** 756–759
66. Toney, M. D., Hohenester, E., Keller, J. W., and Jansonius, J. N. (1995) *J. Mol. Biol.* **245,** 151–179
67. Wilbanks, S. M., and McKay, D. B. (1995) *J. Biol. Chem.* **270,** 2251–2257
68. Villeret, V., Huang, S., Fromm, H. J., and Lipscomb, W. N. (1995) *Proc. Natl. Acad. Sci. U. S. A.* **92,** 8916–8920
69. Rhee, S., Parris, K. D., Ahmed, S. A., Miles, E. W., and Davies, D. R. (1996) *Biochemistry* **35,** 4211–4221
70. Ottemann, K. M., Xiao, W., Shin, Y. K., and Koshland, D. E., Jr. (1999) *Science* **285,** 1751–1754
71. Yu, E. W., and Koshland, D. E., Jr. (2001) *Proc. Natl. Acad. Sci. U. S. A.* **98,** 9517–9520
72. McGrath, M. E., Vasquez, J. R., Craik, C. S., Yang, A. S., Honig, B., and Fletterick, R. J. (1992) *Biochemistry* **31,** 3059–3064
73. Pletnev, V. Z., Zamolodchikova, T. S., Pangborn, W. A., and Duax, W. L. (2000) *Proteins* **41,** 8–16
74. Fuentes-Prior, P., Iwanaga, Y., Huber, R., Pagila, R., Rumennik, G., Seto, M., Morser, J., Light, D. R., and Bode, W. (2000) *Nature* **404,** 518–525
75. Esmon, C. T. (2003) *Chest* **124,** 26S–32S
76. Friedrich, R., Panizzi, P., Fuentes-Prior, P., Richter, K., Verhamme, I., Anderson, P. J., Kawabata, S., Huber, R., Bode, W., and Bock, P. E. (2003) *Nature* **425,** 535–539
77. van de Locht, A., Bode, W., Huber, R., Le Bonniec, B. F., Stone, S. R., Esmon, C. T., and Stubbs, M. T. (1997) *EMBO J.* **16,** 2977–2984
78. Banner, D. W. (1997) *Thromb. Haemostasis* **78,** 512–515
79. Sichler, K., Banner, D. W., D'Arcy, A., Hopfner, K. P., Huber, R., Bode, W., Kresse, G. B., Kopetzki, E., and Brandstetter, H. (2002) *J. Mol. Biol.* **322,** 591–603
80. Gelin, B. R., Lee, A. W., and Karplus, M. (1983) *J. Mol. Biol.* **171,** 489–559
81. Di Cera, E., Dang, Q. D., and Ayala, Y. M. (1997) *Cell. Mol. Life Sci.* **53,** 701–730
82. Gibbs, C. S., Coutre, S. E., Tsiang, M., Li, W. X., Jain, A. K., Dunn, K. E., Law, V. S., Mao, C. T., Matsumura, S. Y., Mejza, S. J., and Leung, L. L. K. (1995) *Nature* **378,** 413–416
83. Dang, Q. D., Guinto, E. R., and Di Cera, E. (1997) *Nat. Biotechnol.* **15,** 146–149
84. Gruber, A., Cantwell, A. M., Di Cera, E., and Hanson, S. R. (2002) *J. Biol. Chem.* **277,** 27581–27584
85. Frisch, C., Fersht, A. R., and Schreiber, G. (2001) *J. Mol. Biol.* **308,** 69–77
86. Di Cera, E. (1998) *Adv. Protein Chem.* **51,** 59–119
87. Ladbury, J. E., Wright, J. G., Sturtevant, J. M., and Sigler, P. B. (1994) *J. Mol. Biol.* **238,** 669–681
88. Bartunik, H. D., Summers, L. J., and Bartsch, H. H. (1989) *J. Mol. Biol.* **210,** 813–828
89. Sanschagrin, P. C., and Kuhn, L. A. (1998) *Protein Sci.* **7,** 2054–2064
90. Liu, L. W., Vu, T. K., Esmon, C. T., and Coughlin, S. R. (1991) *J. Biol. Chem.* **266,** 16977–16980
91. Colwell, N. S., Blinder, M. A., Tsiang, M., Gibbs, C. S., Bock, P. E., and Tollefsen, D. M. (1998) *Biochemistry* **37,** 15057–15065
92. Verhamme, I. M., Olson, S. T., Tollefsen, D. M., and Bock, P. E. (2002) *J. Biol. Chem.* **277,** 6788–6798
93. Le Bonniec, B. F., and Esmon, C. T. (1991) *Proc. Natl. Acad. Sci. U. S. A.* **88,** 7371–7375
94. Colombo, M. F., Rau, D. C., and Parsegian, V. A. (1992) *Science* **256,** 655–659
95. McGee, M., and Wagner, W. D. (2003) *Arterioscler. Thromb. Vasc. Biol.* **23,** 1921–1927
96. Huntington, J. A., and Esmon, C. T. (2003) *Structure* (*Camb.*) **11,** 469–479
97. Carter, W. J., Myles, T., Gibbs, C. S., Leung, L. L., and Huntington, J. A. (2004) *J. Biol. Chem.* **279,** 26387–26394
98. Landis, B. H., Koehler, K. A., and Fenton, J. W., II (1981) *J. Biol. Chem.* **256,** 4604–4610
99. Vindigni, A., and Di Cera, E. (1996) *Biochemistry* **35,** 4417–4426
100. Krishnan, R., Sadler, J. E., and Tulinsky, A. (2000) *Acta Crystallogr. Sect. D Biol. Crystallogr.* **56,** 406–410
101. Guinto, E. R., and Di Cera, E. (1997) *Biophys. Chem.* **64,** 103–109
102. Morris, A. L., MacArthur, M. W., Hutchinson, E. G., and Thornton, J. M. (1992) *Proteins* **12,** 345–364